

PAPER

[View Article Online](#)
[View Journal](#) | [View Issue](#)Cite this: *Dalton Trans.*, 2019, **48**, 7388Received 4th February 2019,
Accepted 25th March 2019

DOI: 10.1039/c9dt00540d

rsc.li/dalton

Design and investigation of photoactivatable platinum(IV) prodrug complexes of cisplatin†

Violet Eng Yee Lee,^{a,b} Chee Fei Chin^a and Wee Han Ang^{*a,b}

Platinum(IV) carboxylate scaffolds have garnered considerable research interest because they can be engineered to function as prodrugs of clinical platinum(II) anticancer drugs. These platinum(IV) prodrug complexes are stable and tunable, and activated by reduction to release their cytotoxic platinum(II) cargo. Here we propose new platinum(IV) prodrug complexes designed to release cisplatin *via* photoreduction upon UV irradiation. The central strategy is to utilise aryl carboxylate ligands on the axial positions of that platinum(IV) scaffold that confer significant UV absorption and would stabilise carboxyl radical formation, thus favouring homolytic Pt–O bond cleavage. We isolated and identified aryl carboxyl radicals *via* spin-trapping and showed that the photoreduced platinum species mirror cisplatin reactivity toward DNA bases, thereby validating the efficacy of this approach.

Introduction

FDA-approved platinum-based anticancer drug cisplatin (cDDP, Fig. 1) is one of the most effective chemotherapeutic agents used in clinic.¹ It displays remarkable curative properties in the treatment of testicular cancer, and is being applied in the first-line therapy against this deadly disease.² Its mechanism of action *in vitro* is mediated by a combination of processes which includes cell entry, activation and DNA-binding *via* the Pt(II) metal centre.^{3–7} cDDP forms mainly intrastrand platinated DNA-adducts with purine nucleosides,^{6–8} and these adducts trigger cellular responses that ultimately result in apoptotic cell death.^{6–9} One major limitation of cDDP-based chemotherapy is the high toxicity and severe side-effects arising from its high reactivity and inability to discriminate between healthy and diseased tissues.^{10,11} This has led to the development of functionalized Pt(IV) prodrug complexes, such as satraplatin, that selectively target cancer cells.^{10,12} These prodrug complexes are activated *via* reduction upon cellular entry to release its cytotoxic Pt(II) cargo.¹³

A strategy that has garnered considerable amount of attention is the selective activation of Pt(IV) prodrugs using light.^{14,15} In this strategy, inert Pt(IV) prodrugs are photoreduced using UV irradiation to cytotoxic Pt(II) species at their

intended site of action. The strategy was first demonstrated by Bednarski and co-workers using diiodo-Pt(IV) complex **1** (Fig. 1).¹⁶ Sadler and co-workers subsequently showed that the replacement of iodide ligands with azide greatly enhanced the photoreductive properties of **2** (Fig. 1) since the dissociated azide ligands irreversibly recombine to dinitrogen and would not be able to reoxidise the Pt(II) centre.¹⁷ In both examples, the equatorial ligands dissociated with concomitant reduction of the Pt(IV) centre. Using radical spin-trapping, Sadler and co-workers demonstrated that the photoreduction of Pt(IV)-azido complex **3** (Fig. 1) proceeded *via* the formation of azidyl radicals.¹⁸ Other reports suggested that non-azido Pt(IV) complexes photoreduce *via* the release of ligands as radical species, although direct evidence were not provided.^{19–21} More recently, Pt(IV) scaffolds conjugated to texaphyrin²² and HDAC inhibitor SubH²³ were applied to deliver cytotoxic Pt(II) payloads *via* photoreduction, although their modes of action were not established.

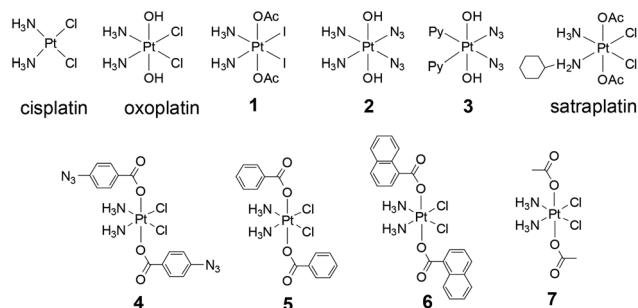


Fig. 1 Molecular structures of cisplatin (cDDP) and other Pt(IV) complexes (Ac = acetate, Py = pyridine).

^aDepartment of Chemistry, National University of Singapore, 3 Science Drive 3, Singapore 117543. E-mail: chmawh@nus.edu.sg

^bNUS Graduate School of Integrative Sciences and Engineering,

National University of Singapore, 21 Lower Kent Ridge Rd, Singapore 119077

†Electronic supplementary information (ESI) available. See DOI: 10.1039/c9dt00540d

We hypothesized that it would be possible to rationally build Pt(IV) complexes that yield cDDP through homolytic photocleavage of the axial Pt–O bonds. Instead of photolabile ligands such as iodide and azide at the equatorial positions, we would retain the cDDP pharmacophore but install axial ligands with significant UV-vis absorption cross-sections that are able to stabilize departing radical species upon dissociation. We surmised that this design would yield prodrugs that could be selectively photoactivated to generate cDDP because these carboxylate ligands would be more photolabile. Based on these considerations, we designed several Pt(IV) scaffolds containing axial aryl ligands and investigated their photoactivation by UV irradiation. We showed that the photoreduction were mediated *via* formation of aryl carboxyl radical intermediates to generate reactive Pt(II) species that bind to 2'-deoxyguanosine-5'-monophosphate (dGMP) in a similar fashion to cDDP.

Results and discussion

Design of UV-activatable Pt(IV) complexes

The azido-benzoate motif was initially selected to prepare photoactivatable Pt(IV) complex **4** (Fig. 1) as a proof of concept. Azido-benzoic acid is a UV crosslinking agent widely used in proteomic photocrosslinking experiments (λ_{ex} at 365 nm). We postulated that nitrene intermediates formed upon photodecomposition could promote reduction of **4**. UV irradiation of **4** at 365 nm proceeded readily with gas evolution, presumably N_2 , with precipitation of an off-white solid. ESI-MS analysis of the precipitate indicated the presence of solvated cDDP adducts amongst other Pt species, presumably due to reaction with reactive nitrenes. This encouraging result prompted the investigation of other easily accessible Pt(IV) scaffolds **5** and **6** (Fig. 1), which were prepared from oxoplatin using established procedures. The naphthoate ligands confer **6** with higher extinction coefficient at 365 nm but with lower aqueous solubility.

Photoreduction of **5** was carried out in acetone by irradiating it at 365 nm with a UV reactor followed by ESI-MS, UV-vis and NMR analyses. Within 5 min, precipitation could be visually observed. TLC analysis indicated the conversion of **5** to a hydrophobic compound exhibiting a similar R_f to benzoic acid, as well as an off-white precipitate. The isolated precipitate exhibited moderate aquatic solubility, unlike **5**, and the ESI-MS spectrum revealed the presence of molecular ions of cDDP and its aggregates (Fig. S1†). Since the Pt coordination sphere is expected to change drastically from Pt(IV) to Pt(II) with the loss of the axial ligands, ^{195}Pt NMR would be an excellent tool to identify the Pt species after UV irradiation. The precipitate exhibited a resonance peak at -2144 ppm which was consistent with the chemical shift of cDDP, in stark contrast to its Pt(IV) precursor (Fig. S2†). The evidence indicated that the azido functional group was not essential for the initiation of Pt(IV) photoreduction.

Time-dependent ^1H NMR studies were conducted to study the effect of UV irradiation at different time intervals (Fig. 2).

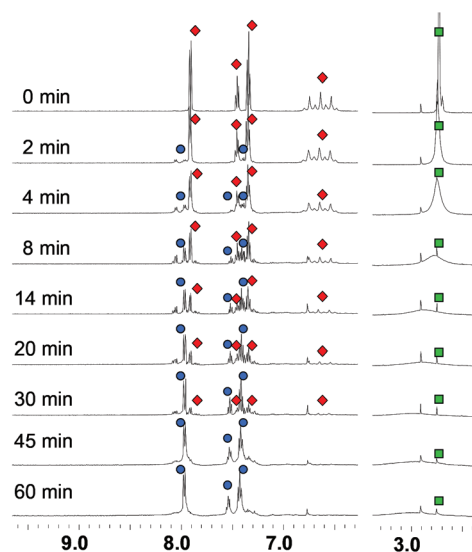


Fig. 2 Effect of UV irradiation at 365 nm on ^1H NMR spectra of **5**; selected regions are shown. From left: Blue circles indicate benzoic acid; Red diamonds indicate the benzoate and NH_3 ligands of **5**; Green squares indicate the residual water present in the solvent.

Upon irradiation, the aromatic and ammine proton resonances of **5** gradually diminished with the appearance of new aromatic peaks assigned to benzoic acid. At the same time, HOD resonance at *ca.* 2.8 ppm, attributable to residual water in the deuterated acetone solvent, diminished in intensity over the course of the reaction. Conversion was complete within 60 min. Based on these observations, we postulated that the irradiation of UV light at 365 nm induced the dissociation of the axial benzoate ligand from the Pt(IV) scaffold *via* homolytic photocleavage of the Pt–O bond, yielding hydrophilic cDDP as precipitate. The benzoyl radical species formed were rapidly quenched by solvent and remained in solution. Similar observations for **6** were made where the appearance of 2-naphthoic acid proton resonances was observed after irradiation (Fig. S3†). In addition, photoreduction of **6** proceeded more rapidly than **5**, with complete conversion of **6** within 10 min of UV irradiation on RP-HPLC (Fig. S4†).

Photoreduction experiments were also carried out on **7**, which lacked aromatic axial ligands. Despite extended irradiation for 2 h, **7** yielded a complex ESI-MS spectrum which suggested hydrolysis of the acetate ligands as well as other low m/z Pt species (Fig. S5†). No distinct cDDP species were observed on ^{195}Pt NMR and ESI-MS. While the possibility of photoreduction at increased intensities or other incident wavelengths cannot be ruled out, the aromatic axial ligands were important to impart UV-activatable properties.

Photoreduction *via* carboxyl radical formation

To validate our hypothesis that benzoyl radical species were formed during the photoreduction of **5**, 5,5-dimethyl-1-pyrroline *N*-oxide (DMPO) was introduced to **5** as a radical spin trap during irradiation at 365 nm. While ESR analyses did not

reveal any spin-trapped adducts, RP-HPLC revealed a new species at $R_t = 24.5$ min formed only in the presence of DMPO (Fig. S6†). Based on time-course experiments, photoreduction was completed in 30 min with the DMPO adduct obtained at 10% yield. The adduct was isolated *via* column chromatography and identified with ESI-MS, ^1H and $^{13}\text{C}\{^1\text{H}\}$ NMR analyses as nitron 5a (Fig. 3 and S7†).

The presence of 5a suggested that benzoyl radical was formed during photoactivation of 5 since DMPO is reactive only toward radical species. It was reported that nitroxide intermediates can be oxidized to a nitron *via* an one-electron oxidation in the presence of an oxidizing agent, which could account for the absence of the ESR-active nitroxide.^{24–26} The spin-trapping experiment using DMPO was repeated for 6 under the same photoactivation conditions, with nitron 6a being isolated and identified (Fig. S8 and S9†). This is the first evidence of carboxyl radical species being formed *via* photoactivation of non-azido Pt(IV) complexes.

Reactivity of Pt complexes toward dGMP after photoactivation

A key determinant of cDDP activity arises from its binding to DNA forming Pt-DNA adducts that interfere with biological processes such as replication and transcription.²⁷ Therefore, we studied the reaction products following photoactivation of 5. In aqueous conditions containing 20% v/v DMF, 5 yielded solvated cDDP adducts which was assigned as $[\text{Pt}(\text{NH}_3)_2(\text{DMF})\text{Cl}]^+$ using ESI-MS analyses. In contrast, irradiation on oxoplatin for extended duration of 2 h did not yield new Pt species. The photoreactivity of 5 toward DNA under different irradiation conditions, using dGMP as a model, was further investigated and compared to cDDP as a control.

In ambient conditions, cDDP reacted readily with dGMP to yield mono-dGMP adducts $[\text{Pt}(\text{NH}_3)_2(\text{dGMP})\text{Cl}]$ as well as bis-dGMP adducts $[\text{Pt}(\text{NH}_3)_2(\text{dGMP})_2]$, consistent with previous reports (Fig. 4).²⁸ Its high reactivity toward guanine bases is well-documented, stemming from the nucleophilic nature of the N⁷-position on the purine ring and cooperative H-bonding interaction between the ammine ligand on cDDP and the exocyclic O⁶-position on guanine.²⁸ Without UV irradiation, 5 was unreactive towards dGMP. However, after exposure to UV irradiation at 365 nm for 1 h, 5 reacted with dGMP to form

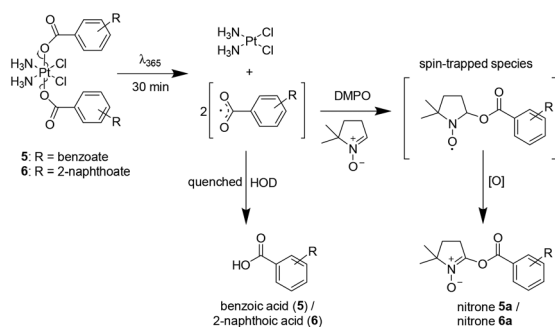


Fig. 3 Proposed mechanism of the spin-trapping of carboxyl radical species with DMPO during photoirradiation of 5 and 6.

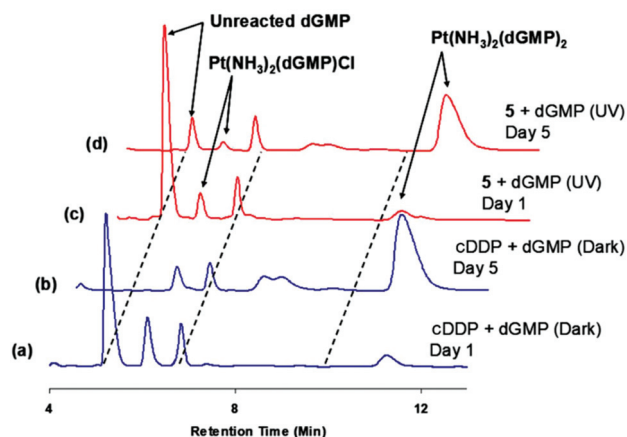


Fig. 4 HPLC chromatograms showing (a) reaction of cDDP with dGMP after 1 d; (b) reaction of cDDP with dGMP after 5 d; (c) reaction of 5 after UV irradiation for 1 h with dGMP for 1 d and (d) reaction of 5 after UV irradiation for 1 h with dGMP for 5 d.

similar mono-dGMP and bis-dGMP adducts as indicated by ESI-MS (Fig. 4).

Analytical HPLC was used to separate the different species formed and peak fractions were collected for ESI-MS (Fig. S10 and S11†). In the case of cDDP, mainly mono-adducts ($R_t = 6.1$ min) were formed after 1 d of treatment while a substantial amount of unreacted dGMP was still present. After prolonged incubation of 5 d, conversion to bis-dGMP adducts ($R_t = 10.9$ min) was almost complete, consistent with slower rate of aquation of the second chloride ligand present in cDDP. In contrast, 5 was unreactive towards dGMP in the dark despite prolonged incubation of 5 d.

Pt(IV) aryl carboxylate complexes as UV-activatable prodrugs

Several implications were drawn from these investigations. Pt(IV) prodrug complexes containing axial aryl carboxylate ligands such as 5 and 6, are stable under ambient conditions but are readily reduced to cDDP upon UV irradiation at 365 nm, as indicated by ESI-MS and $^{195}\text{Pt}\{^1\text{H}\}$ NMR. The drastic change in hydrophobicity resulted in the precipitation of hydrophilic cDDP from organic media, which was isolated and characterised. Cleavage of the axial ligands occurred *via* formation of radical carboxyl species, which were spin-trapped, isolated and characterised as the respective nitron adducts. Photoreduction was also feasible in aqueous media and reactivity towards dGMP could be uncaged after UV irradiation. In the absence of these aryl carboxylate ligands, photoreduction did not occur. We therefore concluded that Pt(IV) carboxylate scaffolds can be rationally designed as photo-activatable prodrugs *via* rational axial ligand design. We also expect that 5 and 6 would be readily reduced to Pt(II) species after cell uptake which would negate the photochemical control afforded by this design.²⁹ Strategies to mitigate this intracellular reduction would be to encase and solubilise the Pt(IV) prodrugs within a UV-permeable hydrophobic protective shell. Salassa *et al.* investigated this strategy and reported that

quantum dot-mediated light activation of Pt(IV) prodrug aided the formation of desired Pt(II) species which makes it advantageous over intracellular reduction.³⁰ Upconversion nanoparticles (UCNPs) is an alternate approach to encase Pt(IV) prodrugs. UCNPs can absorb near-IR light for deeper tissue penetration and emit UV light for photoactivation of the Pt(IV) prodrugs, granting UCNPs-Pt(IV) greater medical application.^{31,32} Lastly, photoreduction would induce a drastic change in hydrophobicity and reduce the solvation of Pt(IV) prodrugs within the shell,³³ paving the way for efficient spatial and temporal release of cDDP triggered by light.

Experimental

Materials and methods

All procedures were carried out without taking precautions to exclude air and moisture, unless otherwise noted. All solvents and chemicals were used as received without further treatment. ¹H, ¹³C{¹H} and ¹⁹⁵Pt{¹H} NMR spectra were recorded on a Bruker AMX 500 spectrometer and the chemical shifts (δ) were internally referenced by the residual solvent signals relative to tetramethylsilane for ¹H, ¹³C{¹H} and K₂PtCl₄ for ¹⁹⁵Pt{¹H} NMR. Mass spectra were measured using a Finnigan MAT LCQ (ESI) spectrometer and Bruker Ultimate 3000 Ion trap (ESI) spectrometer. RP-HPLC was performed using Agilent 1200 DAD with a Phenomenex Luna C18 column (5 μm, 100 Å, 250 mm × 4.6 mm). The HPLC system consisted of a vacuum degasser (Agilent model G1322A), a quaternary pump (Agilent model G1311A), an autosampler (Agilent model G1329A), a thermostated column compartment (Agilent model G1316A) and a diode array detector (Agilent model G1315A). UV spectra were recorded on a Shimadzu UV-1800 UV spectrophotometer using 1 cm path-length cuvettes. Oxoplatin,^{34a} **5**,^{34b} and **7**,^{34c} were prepared and purified according to literature procedures.

Synthesis of 4-azidobenzoyl chloride

In a Schlenk flask, SOCl₂ (2 mL) was added under N₂ to 4-azidobenzoic acid (300 mg, 1.85 mmol). The flask was fitted with a reflux condenser and the reaction mixture was heated at 70 °C for 30 min. SOCl₂ was removed under reduced pressure and the resulting residue was washed with dry ether (3 × 5 mL) and dried under vacuum, affording the product as white powder and used without further purification. ¹H NMR (CDCl₃, 300 MHz): δ 8.05 (d, 2H, Ar-H), 7.08 (d, 2H, Ar-H) ppm. ¹³C NMR (CDCl₃-d₃, 75.4 MHz): 167.5 (s, CO), 148.0, 133.9, 129.9, 119.8 (s, Ar-C) ppm.

Synthesis of *cis,cis,trans*-Pt(NH₃)₂Cl₂(CO₂C₆H₄N₃)₂ **4**

4-Azidobenzoyl chloride (335 mg, 1.85 mmol) was dissolved in dry THF. Pyridine (0.5 mL) was added to the reaction mixture, followed by the addition of oxoplatin (20 mg, 0.07 mmol). The reaction mixture was refluxed for 12 h. The reaction mixture was cooled to r.t. and filtered. The solvent of the filtrate was removed under vacuum. The residue was washed with water (2 × 5 mL), ether (3 × 5 mL) and then with chloroform (1 × 5 mL).

The remaining residue was dried under reduced pressure to give **4** (18.4 mg, 42%). ¹H NMR (DMSO-*d*₆, 300 MHz): δ 7.92 (d, 4H, Ar-H), 7.18 (d, 4H, Ar-H), 6.75 (br, s, 6H, NH₃) ppm. ¹³C {¹H} NMR (DMSO-*d*₆, 75.4 MHz): 172.4 (s, CO), 142.7, 131.2, 129.6, 118.5 (s, Ar-C) ppm. ¹⁹⁵Pt{¹H} NMR (DMSO-*d*₆, 107.62 MHz): 1172.98 ppm. ESI-MS: *m/z* = 622.8 [M – H][–].

Synthesis of *cis,cis,trans*-Pt(NH₃)₂Cl₂(CO₂C₆H₅)₂ **5**

Pyridine (0.5 mL, 6.19 mmol) was added dropwise to benzoyl chloride (0.5 mL, 3.90 mmol) in acetone (5 mL) and stirred for 15 min. Oxoplatin (50 mg, 0.15 mmol) was then added and the mixture was reflux for 4 h. Excess water (20 mL) was added to quench the reaction, and the reaction mixture was filtered. The precipitate was triturated in diethyl ether (3 × 10 mL), filtered and washed with more water to remove the pyridinium salt. The remaining residue was dried under reduced pressure to give **5** as an off-white solid (20 mg, 25%). ¹H NMR (acetone-*d*₆, 500 MHz): δ 7.99 (d, 4H, Ar-H), 7.54 (t, 2H, Ar-H), 7.41 (t, 4H, Ar-H), 6.70 (m, 6H, NH₃, ¹J_{HN} = 53.6 Hz, ²J_{HPT} = 54.3 Hz) ppm. ¹⁹⁵Pt{¹H} NMR (acetone-*d*₆, 107.62 MHz): 1110.76 ppm. ESI (MS): *m/z* = 540.9 [M – H][–].

Synthesis of *cis,cis,trans*-Pt(NH₃)₂Cl₂(CO₂C₁₀H₇)₂ **6**

Pyridine (773 μL, 9.60 mmol) was added dropwise to 2-naphthoyl chloride (1.14 g, 6.00 mmol) in acetone (6 mL). Oxoplatin (100 mg, 0.30 mmol) was added and the mixture was reflux for 4 h, then filtered to remove any solid residue. Hexane (15 mL) was added to precipitate the desired product. The precipitate was triturated in diethyl ether (3 × 10 mL), filtered and washed with more water to remove the pyridinium salt. The remaining residue was dissolved in THF and reprecipitated with hexane (15 mL). The solid was dried under reduced pressure to give **6** as an off-white solid (24 mg, 12%). ¹H NMR (400 MHz, acetone-*d*₆) δ 8.57 (s, 2H), 8.10–8.03 (m, 4H), 7.97 (d, *J* = 7.9 Hz, 2H), 7.93 (d, *J* = 8.6 Hz, 2H), 7.65–7.55 (m, 4H), 6.98–6.66 (m, 6H) ppm. ¹⁹⁵Pt{¹H} NMR (DMSO-*d*₆, 107.62 MHz): 1193.15 ppm. ESI-MS: *m/z* = 641.0 [M – H][–].

Photoactivation studies

DMPO (16 eq.) was added to **5** (1 eq.) and **6** (1 eq.) in acetone, respectively. The reaction mixtures were irradiated in the UV reactor (365 nm, 9.21 mW cm^{–2}) for 30 min. Samples were collected at regular time intervals for HPLC analysis. The eluents were MeCN and water, and the elution condition was 20% MeCN to 90% MeCN from 0 to 40 min.

Spin-trapping studies

DMPO (16 eq.) was added to **5** (1 eq.) and **6** (1 eq.) in acetone, respectively. The reaction mixtures were irradiated in the UV reactor (365 nm, 9.21 mW cm^{–2}) for 30 min and filtered. The filtrate was washed with aqueous NaHCO₃, dried with Na₂SO₄ and dried *in vacuo*. The residue was purified by column chromatography to yield nitrones **5a** and **6a**.

5a: ¹H NMR (500 MHz, CDCl₃) δ 8.11 (dd, *J* = 5.0, 4.3 Hz, 2H), 7.64 (m, 1H), 7.49 (t, *J* = 7.6 Hz, 2H), 2.51 (t, *J* = 7.8 Hz, 2H), 2.09 (t, *J* = 7.8 Hz, 2H), 1.36 (s, 6H) ppm. ¹³C NMR

(126 MHz, CDCl₃) δ 169.59, 163.83, 134.05, 130.18, 128.65, 126.99, 61.26, 31.05, 26.21, 25.26 ppm. ESI-MS: m/z = 233.9 [M + H]⁺.

6a: ¹H NMR (500 MHz, CDCl₃) δ 8.71 (s, 1H), 8.09 (dd, J = 8.6, 1.6 Hz, 1H), 7.98 (d, J = 8.2 Hz, 1H), 7.93 (d, J = 8.8 Hz, 1H), 7.90 (d, J = 8.3 Hz, 1H), 7.64 (t, J = 7.5 Hz, 1H), 7.60–7.56 (m, 1H), 2.54 (t, J = 7.8 Hz, 2H), 2.14–2.10 (t, J = 7.8 Hz, 2H), 1.40 (s, 6H) ppm. ¹³C NMR (126 MHz, CDCl₃) δ 172.09, 169.71, 164.06, 135.97, 132.11, 129.50, 128.90, 128.53, 127.86, 126.98, 125.21, 61.37, 31.92, 31.06, 29.69 ppm. ESI-MS: m/z = 284.0 [M + H]⁺.

dGMP binding studies after photoreduction

The eluents used were 10 mM NH₄OAc and MeOH. The elution gradient was 5% MeOH to 7% MeOH from 0 to 20 min. The eluted peaks were collected at R_t of 6.1 min and 10.9 min for mono-dGMP adduct [Pt(NH₃)₂(dGMP)Cl] and bis-dGMP adduct [Pt(NH₃)₂(dGMP)₂], respectively, as analysed by ESI-MS (Fig. S10 and S11[†]).

Conclusions

In summary, we report a new class of Pt(IV) complexes containing aryl carboxylate ligands designed as UV-activatable prodrugs. The carboxylate ligands were positioned at the axial sites, in contrast to other examples, with the goal of stabilising radical carboxyl species after irradiation. We demonstrated that photoinduced ligand dissociation occurs *via* formation of aryl carboxyl radicals and that reactive Pt(II) species mirroring cDDP reactivity was formed. We are optimistic that by further tuning the nature of the axial carboxylate ligands, the strategy can be extended to access other Pt(IV) constructs that would generate cDDP across a wider range of the electromagnetic spectrum.

Conflicts of interest

There are no conflicts to declare.

Acknowledgements

We acknowledge financial support from Singapore Ministry of Education (R143-000-A53-114). V. E. Y. L. acknowledges scholarship and support from NUS Graduate School for Integrative Sciences and Engineering (NGS).

Notes and references

- L. Kelland, *Nat. Rev. Cancer*, 2007, **7**, 573.
- A. Horwich, J. Shipley and R. Huddart, *Lancet*, 2006, **367**, 754.
- Y. Jung and S. J. Lippard, *Chem. Rev.*, 2007, **107**, 1387.
- D. Wang and S. J. Lippard, *Nat. Rev. Drug Discovery*, 2005, **4**, 307.
- S. Dasari and P. B. Tchounwou, *Eur. J. Pharmacol.*, 2014, **740**, 364.
- D. A. Tolan, Y. K. Abdel-Monem and M. A. El-Nagar, *Appl. Organomet. Chem.*, 2019, **33**, e4763.
- Z. Wang, Z. Deng and G. Zhu, *Dalton Trans.*, 2019, **48**, 2536.
- S. Dilruba and G. V. Kalayda, *Cancer Chemother. Pharmacol.*, 2016, **77**, 1103.
- O. Pinato, C. Musetti and C. Sissi, *Metallomics*, 2014, **6**, 380.
- (a) W. H. Ang, I. Khalaila, C. S. Allardyce, L. Juillerat-Jeanneret and P. J. Dyson, *J. Am. Chem. Soc.*, 2005, **127**, 1382; (b) S. Dhar, F. X. Gu, R. Langer, O. C. Farokhzad and S. J. Lippard, *Proc. Natl. Acad. Sci. U. S. A.*, 2008, **105**, 17356; (c) M. Galanski and B. K. Keppler, *Anticancer Agents Med. Chem.*, 2007, **7**, 55.
- R. Oun, Y. E. Moussa and N. J. Wheate, *Dalton Trans.*, 2018, **47**, 6645.
- C. N. Sternberg, P. Whelan, J. Hetherington, B. Paluchowska, P. H. T. J. Slee, K. Vekemans, P. Van Erps, C. Theodore, O. Koriakine, T. Oliver, D. Lebowitz, M. Debois, A. Zurlo and L. Collette, *Oncology*, 2005, **68**, 2.
- M. D. Hall and T. W. Hambley, *Coord. Chem. Rev.*, 2002, **232**, 49.
- F. S. Mackay, J. Woods, H. Moseley and P. J. Sadler, *Br. J. Dermatol.*, 2005, **152**, 857.
- L. Cubo, A. M. Pizarro, A. G. Quiroga, L. Salassa, C. Navarro-Ranninger and P. J. Sadler, *J. Inorg. Biochem.*, 2010, **104**, 909.
- N. A. Kratochwil, M. Zabel, K. J. Range and P. J. Bednarski, *J. Med. Chem.*, 1996, **39**, 2499.
- P. Müller, B. Schröder, J. A. Parkinson, N. A. Kratochwil, R. A. Coxall, A. Parkin, S. Parsons and P. J. Sadler, *Angew. Chem., Int. Ed.*, 2003, **42**, 335.
- J. S. Butler, J. A. Woods, N. J. Farrer, M. E. Newton and P. J. Sadler, *J. Am. Chem. Soc.*, 2012, **134**, 16508.
- L. A. Wickramasinghe and P. R. Sharp, *Inorg. Chem.*, 2014, **53**, 11812.
- L. A. Wickramasinghe and P. R. Sharp, *Organometallics*, 2015, **34**, 3451.
- T. A. Perera, M. Masjedi and P. R. Sharp, *Inorg. Chem.*, 2014, **53**, 7608.
- T. Grégory, J. F. Arambula, Z. H. Siddik and J. L. Sessler, *Chem. – Eur. J.*, 2014, **20**, 8942.
- J. Kasparkova, H. Kostrhunova, O. Novakova, R. Křikavová, J. Vančo, Z. Trávníček and V. Brabec, *Angew. Chem., Int. Ed.*, 2015, **54**, 14478.
- V. Maurel, J.-L. Ravanat and S. Gambarelli, *Rapid Commun. Mass Spectrom.*, 2006, **20**, 2235.
- B.-Z. Zhu, G.-Q. Shan, C.-H. Huang, B. Kalyanaraman, L. Mao and Y.-G. Du, *Proc. Natl. Acad. Sci. U. S. A.*, 2009, **106**, 11466.
- L. J. Berliner, *Appl. Magn. Reson.*, 2009, **36**, 157.
- J. D. Gralla, S. Sasse-Dwight and L. G. Poljak, *Cancer Res.*, 1987, **47**, 5092.
- U. Warnke, C. Rappel, H. Meier, C. Kloft, M. Galanski, C. G. Hartinger, B. K. Keppler and U. Jaehde, *ChemBioChem*, 2004, **5**, 1543.

- 29 S. Q. Yap, C. F. Chin, A. H. H. Thng, Y. Y. Pang, H. K. Ho and W. H. Ang, *ChemMedChem*, 2016, **12**, 300.
- 30 I. Infante, J. M. Azpiroz, N. G. Blanco, E. Ruggiero, J. M. Ugalde, J. C. Mareque-Rivas and L. Salassa, *J. Phys. Chem. C*, 2014, **118**, 8712.
- 31 S. Perfahl, M. M. Natile, H. S. Mohamad, C. A. Helm, C. Schulzke, G. Natile and P. J. Bednarski, *Mol. Pharmaceutics*, 2016, **13**, 2346.
- 32 E. Ruggiero, J. Hernández-Gil, J. C. Mareque-Rivas and L. Salassa, *Chem. Commun.*, 2015, **51**, 2091.
- 33 (a) J. Li, S. Q. Yap, C. F. Chin, G. Pastorin and W. H. Ang, *Chem. Sci.*, 2012, **3**, 2083; (b) S. L. Yoong, B. S. Wong, Q. L. Zhou, C. F. Chin, J. Li, T. Venkatesan, H. K. Ho, V. Yu, W. H. Ang and G. Pastorin, *Biomaterials*, 2014, **35**, 748; (c) C. F. Chin, S. Q. Yap, J. Li, G. Pastorin and W. H. Ang, *Chem. Sci.*, 2014, **5**, 2265.
- 34 (a) R. J. Brandon and J. C. Dabrowiak, *J. Med. Chem.*, 1984, **27**, 861; (b) W. H. Ang, S. Pilet, R. Scopelliti, L. Juillerat-Jeanneret and P. J. Dyson, *J. Med. Chem.*, 2005, **48**, 8060; (c) L. Chen, P. F. Lee, J. D. Ranford, J. J. Vittal and S. Y. Wong, *J. Chem. Soc., Dalton Trans.*, 1999, 1209.